



Future “local climate zone” spatial change simulation in Greater Bay Area under the shared socioeconomic pathways and ecological control line

Guangzhao Chen^{a,c}, Jing Xie^{b,*}, Wenhao Li^a, Xinwei Li^b, Lamuel Chi Hay Chung^b, Chao Ren^b, Xiaoping Liu^a

^a School of Geography and Planning, Sun Yat-sen University, Guangzhou, China

^b Faculty of Architecture, The University of Hong Kong, Hong Kong, China

^c Institute of Future Cities, The Chinese University of Hong Kong, Hong Kong, China

ARTICLE INFO

Keywords:

Local climate zone
Land-use change simulation
SSP scenarios
City
Google earth engine
The greater bay area

ABSTRACT

Scenario-based land use/land cover change (LUCC) simulation can explore different possibilities in the future for decision-making on city development. However, the current LUCC research in urban-rural areas still lacks support for local climate change research due to unmatched scenario settings and simplified land coverage classification. We thus adopt the local climate zone (LCZ) scheme, which includes more detailed 18 land types, to explore future LUCC in the Guangdong-Hong Kong-Macao Greater Bay Area (GBA) under the latest Intergovernmental Panel on Climate Change (IPCC) scenario, the shared socioeconomic pathways (SSPs), with different policy constraints. First, we produce a 100-m spatial resolution LCZ map of the GBA in 2020, which achieves an accuracy with Kappa = 0.876. Then, we carry out an LCZ simulation by adopting the Global Change Analysis Model (GCAM) and Future Land Use Simulation Model (FLUS) from 2020 to 2100 under the SSPs. The results show that LCZ projections appropriately reflect different land responses under different SSPs and the contrastive LCZ spatial changes among different cities even under the same scenario. Ecological protection is a crucial goal in the development plan of the Chinese government. Thus, we add the ecological control lines to protect ecological land under SSPs. This protection is pronouncedly reflected in ecological land within built-up areas in central cities and ecological land around urban areas in fringe cities. This study is the first test of LCZ projection under SSPs. The study findings could serve as an application potential for urban planning, urban climate and mega-city studies globally.

1. Introduction

Since the Industrial Revolution, human activities have increasingly affected the environment, including climate [1]. There is a conclusive evidence shows that, since the end of the 19th century, the global surface temperature has risen by 0.9 °C [1]. It has been proven that land use/land cover change (LUCC) is one of the crucial factors profoundly affecting the climate at both a regional and a global scale, such as surface temperature [2], carbon emissions [3] extreme weather [4]. Simultaneously, human policies can significantly affect land change, such as urban planning, land management, afforestation, deforestation, and agricultural expansion [5–9]. To address the challenges of climate change and create a more liveable future, countries worldwide have formulated sustainable goals and plans that can be achieved through implementable policies. For instance, in 2015, countries in the United

Nations signed the Sustainable Development Goals (SDGs) to be reached by 2030, which includes 17 SDGs and 169 targets [10]. At the national level, taking China as an example, China has made sustainable development one of its government's crucial strategies and is committed to building a sustainable society in its five-year development plan [11]. These goals and plans will be transformed into different local policies on city development, directly affecting LUCC.

To explore the impact of policies on LUCC, many researchers have performed land change simulations under different policy-pathway scenarios. Some of these simulation studies only focus on urban area [12], while others consider different land types [13]. In many local and regional studies, the basis for scenarios setting is often relatively straightforward. The popular future scenarios set up and adopted by researchers include development along the historical trajectory, cropland protection policies, ecological zone protection policies, and energy

* Corresponding author. Knowles Building, The University of Hong Kong, Pokfulam Road, Hong Kong, China.

E-mail address: xiej412@hku.hk (J. Xie).

<https://doi.org/10.1016/j.buildenv.2021.108077>

Received 30 January 2021; Received in revised form 8 June 2021; Accepted 8 June 2021

Available online 27 June 2021

0360-1323/© 2021 Elsevier Ltd. All rights reserved.

consumption [14–18]. However, the parameters for setting these scenarios are relatively simple, and the standards for setting parameters are also relatively arbitrary, these limitations hence restrict the comparability between different studies and the versatility of products.

To meet the universality of climate change scenarios, Coupled Model Intercomparison Project Phase 6 (CMIP6) proposes a new scenario framework, the shared socioeconomic pathways (SSPs), for global climate and LUCC researchers. This framework has also been adopted by the Intergovernmental Panel on Climate Change (IPCC) [19]. The SSPs is a scenario framework that considers socioeconomic, technology, and policies, which also corresponds to certain climate consequences [20]. There are five scenarios of the SSPs. SSP1 is a scenario of sustainable development, taking the green road [21]. SSP3 is a road of regional competition, reducing international trade with slow economic development [22]. SSP2 is the middle road between SSP1 and SSP3 [23]. SSP4 is the road of division, in which the developed regions will be well developed and managed, while the backward regions are the opposite [24]. SSP5 is the road of fossil-fuelled development, which yields rapid economic growth but emits more carbon [25].

However, there is still a lack of land-cover change research based on SSPs. For example, Popp et al. [26] only projected the land area of different regions under the SSPs but lacked spatial details. The official land cover data set of CMIP6, LUH2 [27], only has a coarse resolution of 0.25°. Chen et al. [28] developed a 1-km resolution projection of future global urban expansion based on SSPs, but their results can only distinguish between urban and non-urban land. Similarly, in the future LUCC simulation of China conducted by Liao et al. [29], urban land is treated as a whole. For researches on urban geographies, such as urban climate, urban energy and urban planning, a single urban land type can not provide sufficient reference information. However, current research mainly focuses on the global and national scales, and there are still gaps in studying the impact of SSPs on land change at the regional scale.

To address urban-rural description inadequacies, a new land classification, local climate zone (LCZ), was proposed [30]. LCZ is a concept developed to depict urban morphology and land surface structure and provide an international standardised land-use and land-cover classification approach for cross-comparison within and between cities [30]. The LCZ scheme was initially designed conceptually at a local scale in urban and rural environments [31,32]. Compared to natural land areas with a higher vegetation coverage ratio, urban areas with a higher impervious surface coverage ratio trap more heat and energy. Therefore, the impervious surface in urban areas will increase the sensible heat flux, which will lead to the urban heat island (UHI) effect [33]. Compared with the general land-use and land-cover classification, LCZ can provide more detailed information about the urban-rural environment.

Besides, LCZ will be a suitable classification for the research gaps in the regional-scale land change research on SSP scenarios, especially in metropolitan areas. Therefore, we choose the Guangdong-Hong Kong-Macao Greater Bay Area (GBA) as the study area. The GBA is one of the regions with the highest degree of openness and the most economic vitality in China, aiming to become a world-class urban agglomeration. Moreover, the Chinese government has elevated the GBA's development to a national strategic position and formulated a particular development plan [34]. The GBA will have a vast potential for growth and a strong driving force for its development into a world-class bay area.

Therefore, in this study, we will carry out an LCZ map at a 100-m scale in 2020 and implement a projection of future LCZ dynamics in a famous metropolitan area, the GBA, under the SSPs. Further, we will explore the impact of the implementation of the local land management policy, the ecological control line, on land change in the context of SSPs. This study may be the world's first projection of the future LCZ under the SSPs at the metropolitan scale.

2. Materials and methods

The flow chart of this study is shown in Fig. 1. It can be divided into three parts: the first is the mapping of LCZ distribution in the GBA in 2020; the second is the forecast of future land demand based on SSPs; the third is the spatial simulation of future LCZ under different SSPs and land management policy constraints.

2.1. Study area

The GBA surrounds the Pearl River's estuary with 56,000 km², including two special administrative regions of Hong Kong and Macao, and nine of Guangdong Province's prefecture-level cities: Guangzhou, Shenzhen, and Foshan Dongguan, Zhongshan, Zhuhai, Huizhou, Jiangmen, and Zhaoqing (Fig. 2). By the end of 2017, the GBA had 72.65 million people and 12% of the national GDP, with a per capita GDP of US \$23,100 [34]. Compared to the world's major bay areas, the New York Bay Area, Tokyo Bay Area, and San Francisco Bay Area, GBA has the largest population and most extensive area [35]. Although the current per capita GDP of the GBA is still far behind that of other major Bay Areas, the GBA has experienced a rapid development process in the past three decades and still shows enormous development potential. In the nine cities in Guangdong Province, their resident population increased by 160%, and their GDP increased by 74 times from 1990 to 2017 [36].

2.2. Data input

(1) Spatial data for future LCZ simulation

Land simulation researchers have proved that land dynamic is closely related to spatial driving factors [37–40]. One of the keys to carry out land change simulation correctly is to select appropriate spatial driving factors to reflect the socioeconomic and physical environment. Therefore, for the urban land types in the LCZ, we chose the spatial driving factors related to the social economy, such as population, road, and points of interest (POI). For the natural land types in the LCZ, we selected spatial driving factors that reflect physical conditions, such as terrain, soil quality, temperature, and precipitation. All the spatial driving factors used in the LCZ simulation in this study are shown in Table S1.

(2) Data for the projection of land-use demands under SSPs

In this study, we used the Global Change Analysis Model (GCAM) model to predict land demands' changes under SSPs. The GCAM model requires global-scale land cover data for calibration, so we chose MODIS land cover data as calibration data for GCAM. Besides, since the GCAM model cannot forecast urban land demand, we refer to the urban land demand data created by Chen et al. [28], which considers the changes in GDP, population, and urbanisation rate under different SSPs to predict the corresponding urban land demands.

(3) Ecological control line

The ecological control line data is crucial for evaluating environmental policy. However, we could hardly find available data on the ecological control line in public databases. Therefore, we used GIS tools and several recognised guidelines to extract the range of GBA's ecological control lines [41]. The specific guidelines are as follows: First, first-level water source protection areas, scenic spots, nature reserves, concentrated areas of basic cropland, natural forests, and country parks. Second, mountain and woodlands with a slope higher than 25°. Third, main rivers, reservoirs, and wetlands. Fourth, ecological corridors and green spaces that maintain the integrity of the ecosystem. Fifth, islands and coastal land areas with ecological protection value. Sixth, other areas that require basic ecological control.

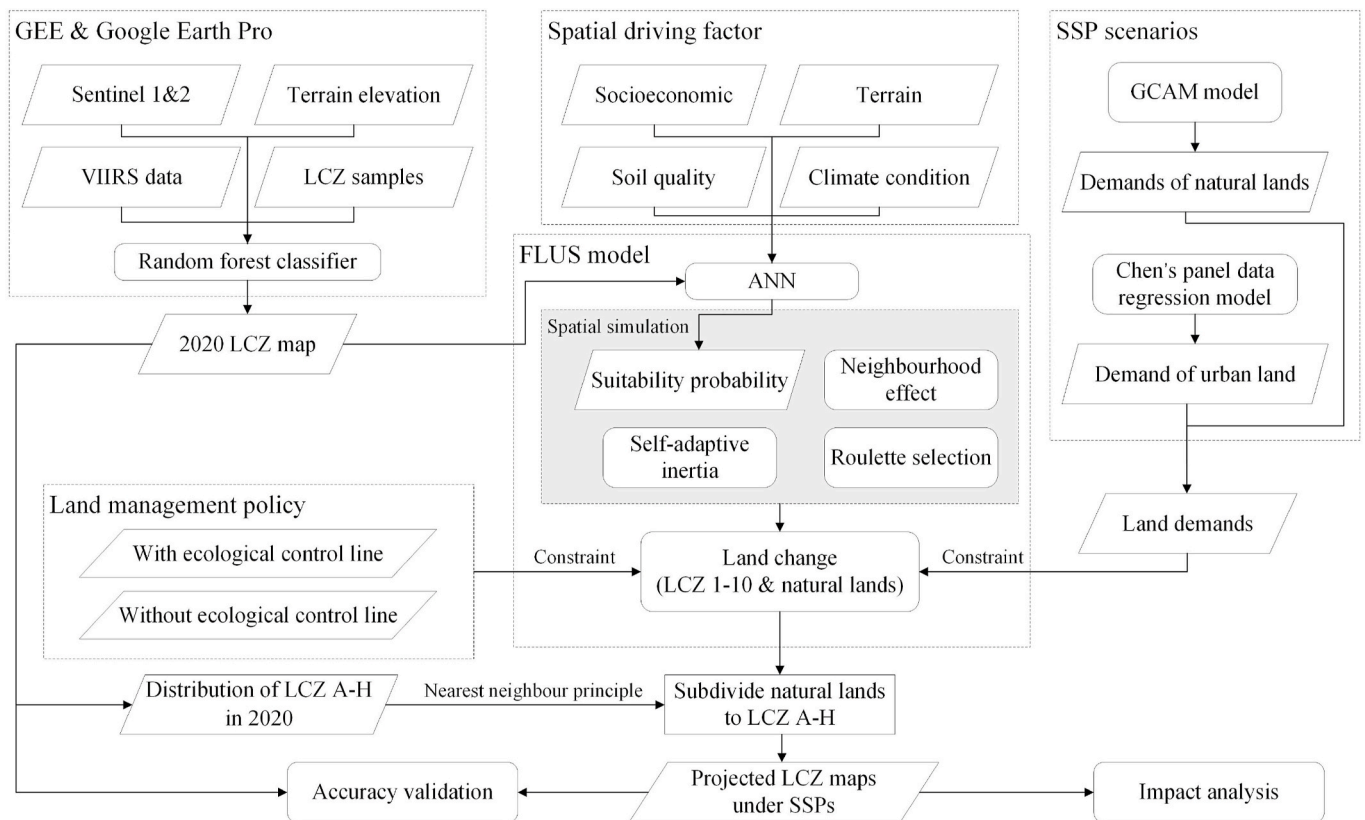


Fig. 1. Flow chart of this study.

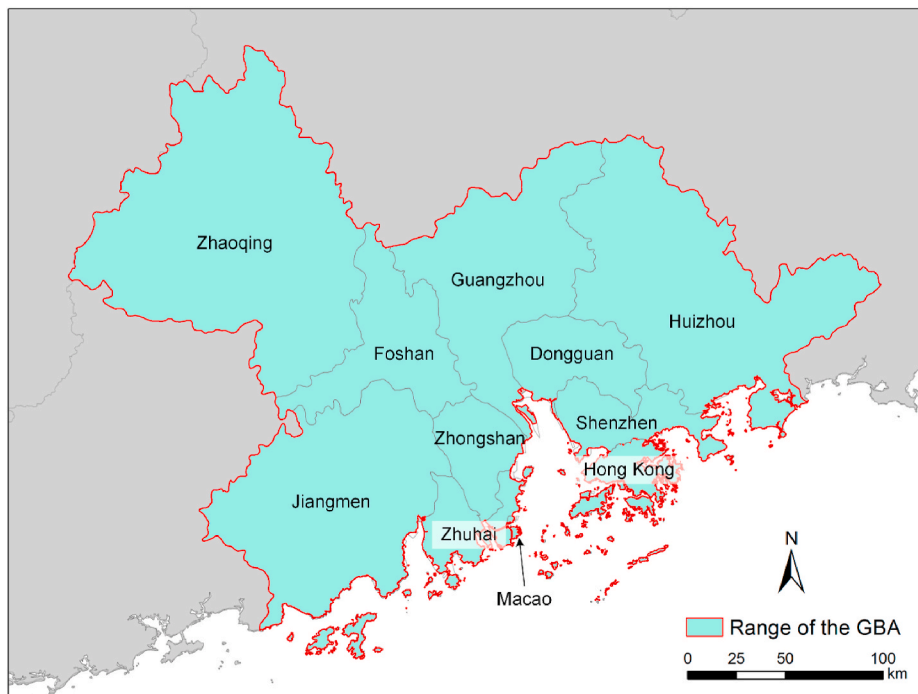


Fig. 2. Location and extent of the Guangdong-Hong Kong-Macao Greater Bay Area (GBA).

2.3. Method of the LCZ classification

Nowadays, more and more open-accessed satellite-based remote sensing images are freely available to the public, such as multispectral and backscatter imageries. It is possible to develop LCZ maps and

monitor urbanisation progress easily and systematically. Our LCZ mapping comprised three key steps: (1) input data-processing using the GEE platform; (2) LCZ samples data (for training and validation) collection using Google Earth Pro; and (3) application of the random forest classifier, as conducted by the LCZ classification of Chung et al.

[42].

First, the Sentinel-1 SAR GRD (C-band Synthetic Aperture Radar Ground Range Detected, log scaling, cloud-free), Sentinel-2 MSI (Multi-spectral Instrument, Level-1C), and VIIRS (Stray Light Corrected Nighttime Day/Night Band Composites Version 1) of the year 2020 and GMTED2010 (Global Multi-resolution Terrain Elevation Data 2010) were clipped within the region-of-interest (i.e. the GBA region) and employed as the primary image sources for mapping LCZ of 2020 in the GBA. All spectral bands of Sentinel-2 MSI after masking off the cloudy pixels, backscatter values (i.e., VV and VH) of Sentinel-1 SAR GRD, “avg_rad” of VIIRS Stray Light, and “be75” (i.e., elevation information) of GMTED2010 were selected as input data for classification.

The second input to the classification were 2144 training samples (Fig. S1) collected across the urban areas and their surrounding areas within the GBA region based on the representative characteristic of LCZ types (Table 1). Sample polygons were digitised and saved as vectorised KMZ format using Google Earth Pro before imported into Google Earth Engine (GEE) platform. Samples were split randomly with 70% samples (1459 samples) as training samples and the remaining 30% samples (685 samples) as validating samples to evaluate the classifier’s performance.

The above satellite images, geospatial data and the 1459 training sample polygons were used to train a random forest classifier in the GEE platform. Random forest is an ensemble classifier operated by constructing multiple decision trees in a training session and assigning the target’s class by majority voting [43]. Each tree in the random forest will spit out a class prediction, and the class with the most votes would become the classifier’s final prediction. We chose this classifier because it can protect each decision tree from individual errors, balance the achieved accuracy and computational performance [44]. The GEE “.smileRandomForest” package was employed to implement the random forest classification. In this study, we set all parameters at the GEE default values, except the n-tree (the number of trees). A grid search of five trees per grid was performed from 1 to 100 trees to determine the optimal number of trees for classification. 80 trees were set as the optimal number of trees for classification according to the error tests in this practice. The LCZ map of the GBA region was then generated for the year 2020 (see Fig. S2).

Table 1
Surface properties of local climate zones (LCZs) simplified from Stewart & Oke [30].

LCZ types	Built and land cover types	Anthropogenic heat flux density ^a	Aspect ratio ^b	Sky view factor ^c	Building surface fraction ^d	Impervious surface fraction ^e	Height of roughness elements ^f
LCZ 1	Compact high-rise	50–300	>2	0.2–0.4	40–60	40–60	>25
LCZ 2	Compact mid-rise	<75	0.75–1.5	0.3–0.6	40–70	30–50	8–20
LCZ 3	Compact low-rise	<75	0.75–1.5	0.2–0.6	40–70	20–40	3–8
LCZ 4	Open high-rise	<50	0.75–1.25	0.5–0.7	20–40	30–40	>25
LCZ 5	Open mid-rise	<25	0.3–0.75	0.5–0.8	20–40	30–50	8–20
LCZ 6	Open low-rise	<25	0.3–0.75	0.6–0.9	20–40	20–40	3–8
LCZ 7	Lightweight low-rise	<35	1–2	0.2–0.5	60–90	<10	2–4
LCZ 8	Large low-rise	<50	0.1–0.3	>0.7	30–50	40–50	3–10
LCZ 9	Sparsely built	<10	0.1–0.25	>0.8	10–20	<20	3–8
LCZ 10	Heavy industry	>300	0.2–0.5	0.6–0.9	20–30	20–40	5–15
LCZ A	Dense trees	0	>1	<0.4	<10	<10	3–30
LCZ B	Scattered trees	0	0.25–0.75	0.5–0.8	<10	<10	3–15
LCZ C	Bush, scrub	0	0.25–1.0	>0.9	<10	<10	<2
LCZ D	Low plants	0	<0.1	>0.9	<10	<10	<1
LCZ E	Bare rock or paved	0	<0.1	>0.9	<10	>90	<0.25
LCZ F	Bare soil or sand	0	<0.1	>0.9	<10	<10	<0.25
LCZ G	Water	0	<0.1	>0.9	<10	<10	–
LCZ H	Wetlands ^g	0	<0.1	>0.9	<10	<10	–

^a Mean annual anthropogenic heat flux density (Wm⁻²) at the local scale. Varies significantly with latitude, season, and population density.

^b Mean height-to-width ratio of street canyons (LCZ 1–7), building spacing (LCZ 8–10), and tree spacing (LCZ A–H).

^c Ratio of the amount of sky hemisphere visible from ground level to that for an unobstructed hemisphere.

^d Proportion of the ground surface with building cover (%).

^e Proportion of the ground surface with impervious cover (rock, paved) (%).

^f Geometric average of building heights (LCZ 1–10) and tree/plant heights (LCZ A–F) (m).

^g Wetlands is an additional LCZ type that adapted the land surface properties of coastal cities in the GBA region.

2.4. Prediction of future LCZ demands of under SSPs

GCAM is one of the well-known integrated assessment models (IAM), which participates in Coupled Model Intercomparison Project Phase 6 (CMIP6) [27,45]. GCAM is a complex system coupled with multiple departments considering political, physical, technological, and spatial detail [46]. Therefore, it can predict the future land use demand under 5 SSP scenarios, taking into account the different storylines of these SSPs. Moreover, it is a rare IAM model that can be downloaded for free, and the parameters of the model can be set as needed [47]. Consequently, we chose the GCAM model to predict future land demand under SSPs. As a global-scale model, this study only needed the global land cover data (MODIS land cover data) of the initial year as input to execute and output the forecast results of land demand.

However, GCAM cannot output forecasts for future urban land demand. Hence, we have to choose another model that can predict future urban land demand. Chen et al. [28] proposed a panel data regression model to predict the future urban land demand under SSPs, which considered socioeconomic factors such as GDP, population, and urbanisation rate. Their results reasonably reflected the trends of urban land demand caused by different SSPs storylines. Therefore, we adopted their forecast of future urban land demand. To be precise, we used their predicted urban land demand trajectory (rate of change) in China under the SSPs to calculate the future urban land demand based on our initial urban land data.

GCAM and Chen’s land classification systems are not consistent with the LCZ. We thus established a reclassification scheme to unify these classifications for space simulation (Table 2). The land types of GCAM, Chen’s, and LCZ were merged and correspond to six classes (forest, shrub, low plants, urban, barren, water). Primarily, the urban land demand was allocated to the urban-type land in the LCZ according to the proportion of them in the initial year.

Since both GCAM and Chen’s models predict China as a whole, and there is a gap in the area of different data in the initial year, we need to calibrate the gap in the area between the GCAM and Chen’s prediction of China and our LCZ product of the Greater Bay Area. The principle of calibration is to maintain the trajectories of various land types provided by GCAM and Chen’s model under SSPs. We used the following formula

Table 2
Land classifications for our simulation based on the GCAM model, LCZ and MODIS.

Our simulation	GCAM	LCZ	MODIS
Urban/LCZ 1–10	Urban	LCZ 1–10	Urban and Built-up Lands
Forest	Forest	LCZ A, LCZ B	Evergreen Needleleaf Forests Evergreen Broadleaf Forests Deciduous Needleleaf Forests Deciduous Broadleaf Forests Mixed Forests
Shrub	Shrubs	LCZ C	Closed Shrublands Open Shrublands
Low plants	Grass	LCZ D	Woody Savannas Savannas Grasslands Croplands Cropland/Natural Vegetation Mosaics
Barren	Tundra Rock and desert	LCZ E, LCZ F	Permanent Snow and Ice Barren
Water	Water	LCZ G, LCZ H	Water Bodies Permanent Wetlands

to execute the calibration:

$$\Delta A_{i,t+1} = \frac{\Delta GA_{i,t+1} \times TAB}{TAC}$$

where, $\Delta A_{i,t+1}$ represents the changing area in the Greater Bay Area of land type i from time t to time $t+1$. $\Delta GA_{i,t+1}$ represents the changing area in China of land type i from time t to time $t+1$ provided by GCAM or Chen's model. TBA means the total area of the Greater Bay Area. TAC means the total area of China.

2.5. Future LCZ simulation by FLUS

To satisfy the simulation needs of multi-land-type and 100-m-resolution, we performed spatial simulations by the FLUS model, which has reliable computing power and accuracy [48]. The software of FLUS is available for free with a user manual at <http://www.geosimulation.cn/FLUS.html>. The FLUS is a CA-based model with two significant improvements. While retaining the essential characteristics of cellular automata (CA), FLUS adopts a roulette selection mechanism and a self-adaptive inertia mechanism [38]. The roulette selection mechanism can realise the complex competition between different land types. Simultaneously, it eliminates the defect that users need to set thresholds subjectively in traditional CA to determine whether the grid changes its status. The adaptive inertia coefficient is an internal parameter that adjusts the simulation speed. It can automatically adjust itself according to the gap between the current land area and the land demand after each iteration so that all land types finally reach their demands.

Each grid is estimated with total probabilities corresponding to each land type in each iteration, and the roulette selection mechanism determines the state of the grid in the next step based on these total probabilities. The formula for calculating the total probability is as follows [48]:

$$TP_{ij} = Pg_{ij} \times neighbor_{ij} \times inertia_j \times cons_{k \rightarrow j}$$

where, TP_{ij} represents the total probability of grid cell i becoming land type j . Pg_{ij} represents the suitability probability of land type j on grid cell i . $neighbor_{ij}$ means the neighborhood effect of land type j around grid cell i , and it is positively related to the number of grids of land type j around grid cell i . $inertia_j$ means the adaptive inertia coefficient of land type j . $cons_{k \rightarrow j}$ represents the constraint of changing from the current land type k to land type j . That is, its value is 0 when such conversion is not allowed, and otherwise, the value is 1. In this study, we neither allow

urban land to convert to non-urban land types nor simulate water changes.

One of the keys to ensuring the simulation's accuracy is the suitability probability. It is estimated in FLUS by the artificial neural network (ANN), considering various spatial driving factors. The adopted spatial driving factors should fully reflect the relevant factors affecting the changes of each land type [40,49]. The FLUS model randomly selected a small number of grids (1%) as sample points and collected the values of the spatial driving factors and the land type in the initial year on these sample points. Then, 70% of the samples were fed into the ANN to train and fit the relationship between spatial driving factors and land type. The remaining 30% of the samples were used to assess the performance of the training of the ANN [48].

Considering the differences in spatial driving factors for urban-type and non-urban-type lands in LCZ, our LCZ simulation and the estimation of suitability probability were divided into two parts accordingly.

The first part was to simulate the spatial changes of the urban-type land in the LCZ (LCZ 1–10). To estimate the suitability probabilities of the urban-type land, we contained relevant spatial driving factors into the ANN, such as population, road, different types of points of interest (POI), and terrain (Table S1). Types of POI included commercial building, retail, hotel, restaurant and entertainment, hospital, school, company, park and square, residential community, governmental organisation, bus station, airport, railway station, and car park. Each of them was evaluated for their kernel density distribution for the ANN training and estimation. With the estimated suitability probabilities, we executed the FLUS model to simulate the spatial change of LCZ 1–10 under SSPs and the constraint of the LCZ demands.

The second part was to simulate the remaining land types (forest, shrub, cropland, barren). Considering that these land types are greatly affected by physical conditions, we added pertinent spatial driving factors when estimating their suitabilities, including climate conditions and soil quality (Table S1). Like the first part, the ANN was trained to estimate the suitabilities and execute the FLUS model to simulate the land use's spatial change. All the spatial driving factors we used are shown in Table S1.

After completing the two parts of the LCZ simulation, we also need to allocate the five land types (forest, shrub, cropland, barren, water) into corresponding the LCZs (LCZ A–H). We further allocated the five land types grid-by-grid to the LCZ closest to them in the initial year according to the nearest neighbour principle and Table 2. For this process, we used the spatial analysis tools provided by ArcGIS software. First, we used the Euclidean Distance tool to calculate the distance of each grid to each type in LCZ A–H in the initial year separately. Then, we used the Raster Calculator tool to convert grids belonging to the simulated five land types into the nearest corresponding LCZ type based on the relationship in Table 2. For example, a simulated forest grid is converted to LCZ A or LCZ B based on the euclidean distance calculated in the previous step. Finally, we mosaiced the simulation results of the first part (LCZ 1–10) and the second part (LCZ A–H) into a complete LCZ prediction product under SSPs.

When performing simulations under the ecological control line constraints, this study only needs to add the ecological control line as a limiting condition and repeat the simulation with FLUS, maintaining the suitabilities and land demand unchanged. Within the extent of the ecological control line, natural land was not allowed to be changed into urban-type LCZs (LCZ 1–10).

3. Results

3.1. Accuracy of the LCZ classification

An independent set of validation samples (i.e., 685 samples) was collected to evaluate LCZ classification results' accuracy (Table S2). By comparing the developed LCZ results with ground truth data, the degree of confusion between the resultant classifications and the ground truth

can be calculated. The assessment results are presented in a confusion matrix. With an overall accuracy of 94.4%, built-up accuracy of 71.0%, and kappa coefficient of 0.876, the quality of the developed LCZ data is acceptable, according to Bechtel et al. [31].

3.2. Accuracy of the LCZ simulation

Fig. 3 shows the LCZ simulation results in each SSP scenario in 2100. In the FLUS model, the suitability probability is the key to simulation accuracy [28,48]. We used the Area Under the Curve (AUC) to reflect the accuracy of the obtained suitability probability (Fig. 4 and Table S3). The AUC of the suitability probabilities of all land types during the simulation has reached an acceptable value. Their average is 0.744, showing that our simulation accuracy is reliable. Among them, barren has the lowest AUC, which is only 0.613. However, it has a limited impact on the simulation results' overall performance because the proportion of barren in the GBA is tiny.

Similarly, LCZ 5 (open midrise) has a relatively low AUC of 0.628. LCZ 5 represents mid-rise building areas with low density. LCZ 5 is also less distributed in the GBA, so it attains a relatively low but acceptable accuracy.

3.3. Differences of LCZ changes between different SSPs

Different LCZs present different demand trajectories in different scenarios. We merged 18 types of LCZ into 5 types to facilitate the display and showed their demand changes in Fig. 5. It indicates that GBA's urban land (LCZ 1–10) demand will continue to rise before the 2040s–2050s but will be frozen after that. The freeze is mainly due to the decline in China's future population in the SSP forecast data [28]. From a scenario perspective, urban land has the largest increase in the SSP5, the fossil-fuelled development path, followed by the SSP1, the green development path. In SSP3, urban land demand is the lowest due to de-globalisation, slow economic development, and low population growth. The changing trends of shrubs (LCZ C), low plants (LCZ D), and barren (LCZ E&F) show a clear negative correlation with urban land. They suffer a significant decrease before the 2050s but have become flat since then.

In addition to the substantial urban expansion, another noticeable feature is the overall growth of forest (LCZ A&B) in SSP4 (Fig. 5). In most scenarios, GBA's forest shows recovery and growth, except for SSP3. In SSP3, the lack of regulation of land changes leads to weak forest restoration. In SSP4, the divided path, the GBA forest areas can get the best recovery and growth because the GBA as the middle and high-income regions can implement the policy of reducing deforestation and strengthening afforestation. Also, SSP1, the green development path, will see evident growth in the forest.

We performed an LCZ simulation on GBA based on the above demand. The simulation results allow us to discover the different land responses of cities in GBA to SSP scenarios. Fig. 6 shows the changes of varying land types in typical GBA cities from 2020 to 2100. Fig. 6 a, b, and c show the land area changes of the core cities in the GBA, Guangzhou, Shenzhen, and Hong Kong. It clearly shows that the land change in core cities is dominated by urban land. The natural land use in core cities will reduce in the future in almost all scenarios. One exception is that Hong Kong achieves forest growth in SSP4 due to the implementation of afforestation policies. Fig. 6-d, e and f show the land area changes of fringe cities in the GBA, Huizhou, Jiangmen, and Zhaoqing. In sharp contrast with the core cities, the forest will expand in the fringe cities in most scenarios, even faster than urban land. Besides, the reduction of low plants is mainly controlled by urban expansion in the core cities, while it is jointly affected by urban and forest in the fringe cities.

In addition to quantitative statistics, we analyse the spatial changes of different land types. We used block statistics to enhance the visualisation to display the land changes within every 5-km grid by 2100 (Figs. 7–9). Fig. 7 shows the spatial changes of forest (LCZ A&B) under different SSPs from 2020 to 2100. Forest has the most significant growth in SSP4 and SSP1. The forest growth is mainly concentrated on the GBA fringe, corresponding to Jiangmen, Zhaoqing, and Huizhou. At the same time, the forest in the central area of the GBA experiences a decrease. In SSP5, where the urban expansion is the most intense, this contrast is even more apparent.

Fig. 8 shows the spatial changes of shrubs (LCZ C) under different SSPs from 2020 to 2100. Shrub occupies less area in GBA, so its change is also slight. Unlike the forest, the shrub changes are more concentrated in

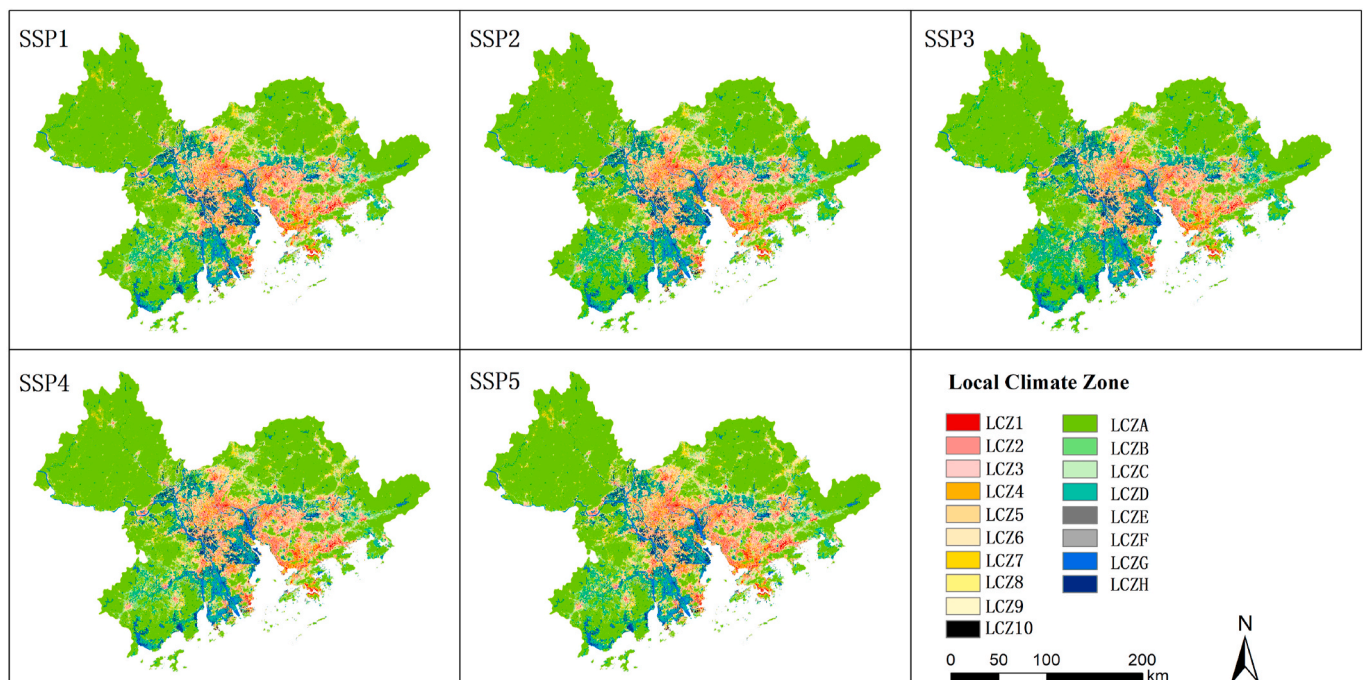


Fig. 3. LCZ simulation results in 2100 in each SSP scenario.

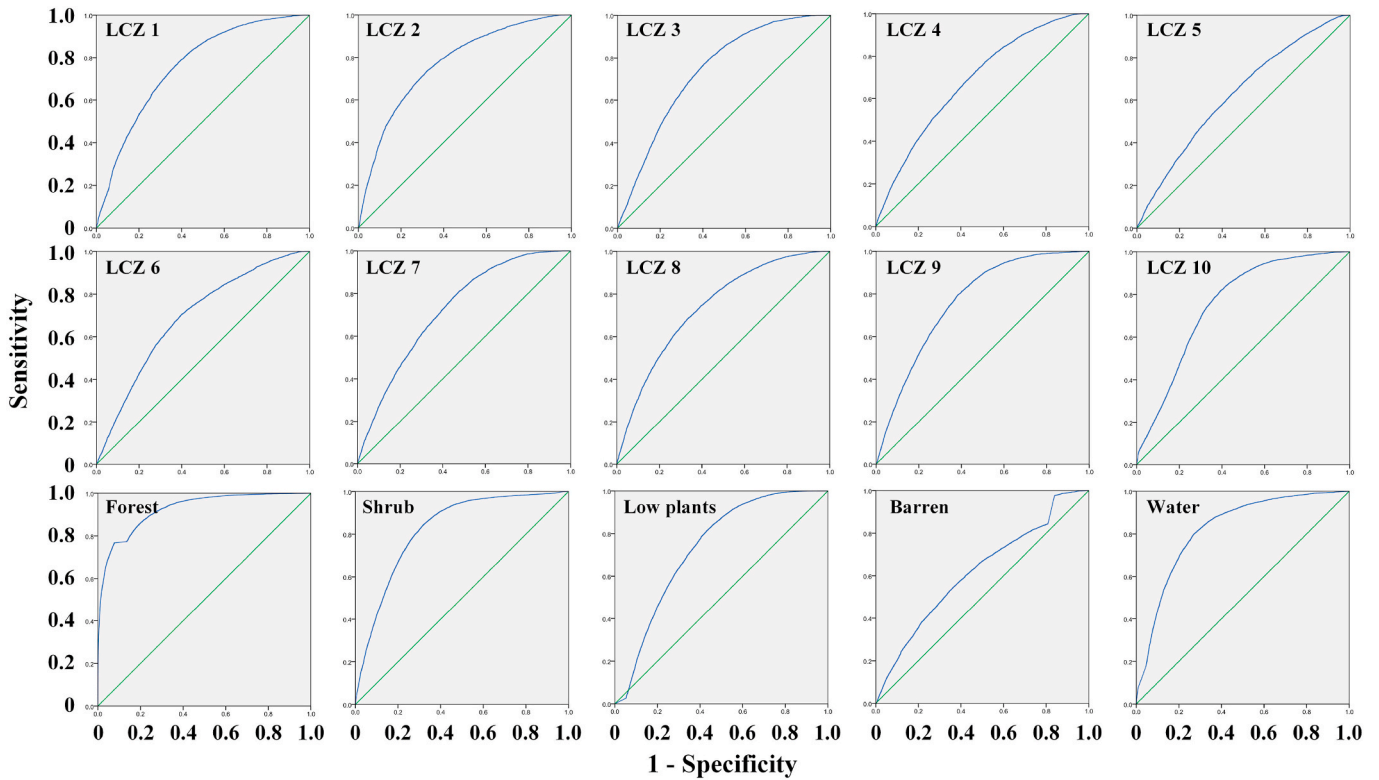


Fig. 4. ROC Curve of the land types in our simulation.

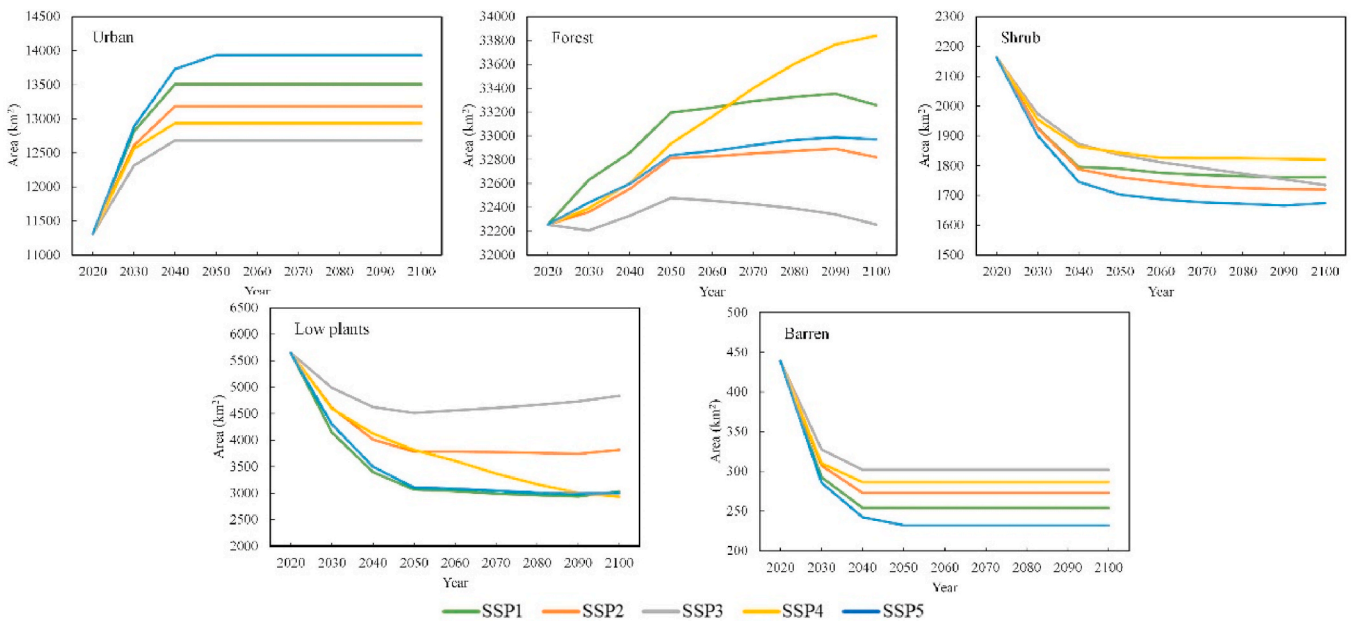


Fig. 5. The land demands of various land types in GBA under the SSPs from 2020 to 2100.

areas close to urban land. However, shrub also tends to decrease in the central area and increase in the periphery.

Low plants (LCZ D) is a considerable land type in GBA. Generally, low plants include two types of land: grassland and farmland. However, since GBA has few grasslands, the low plants (LCZ D) in GBA are almost representing farmland. Fig. 9 shows the spatial changes of low plants (LCZ D) under different SSPs from 2020 to 2100. In SSP3, the low plants' changes are the slightest, it is due to the low growth of urban land due to economic depression and population decline, and the non-

implementation of afforestation policies. In the remaining four SSPs, low plants experience a wide range of reductions in both central and peripheral areas. Comparing to Fig. 7, it can be found that the amount of reductions in low plants are due to forest encroachment.

Simulation results also depict the spatial changes in urban LCZs. Urban LCZs contain ten sub-types, and the area of each type is so small that it is difficult to visualise their changes. Therefore, the SSP2 scenario is taken as an example as it is considered to be the scenario closest to the historical trajectory. A table is also used to statistically present the city-

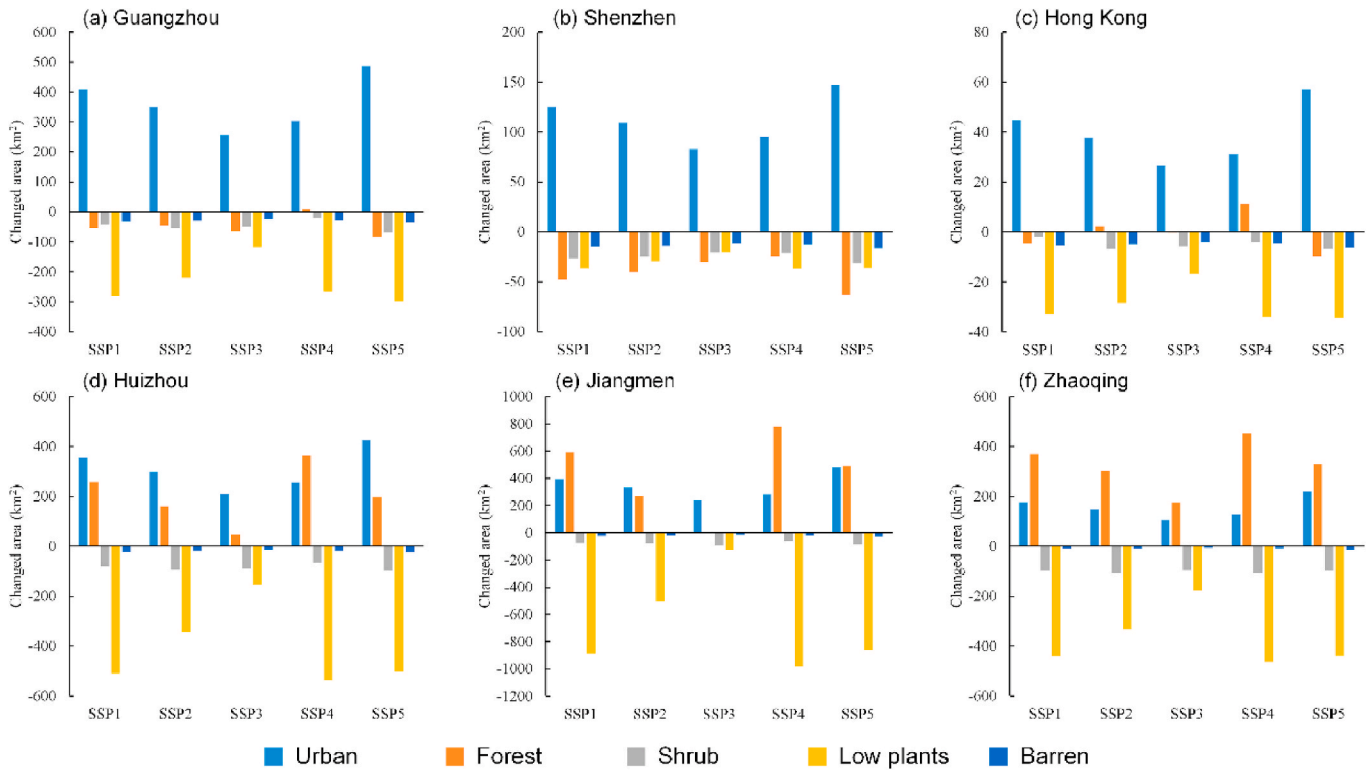


Fig. 6. The area change of different land types in typical GBA cities from 2020 to 2100.

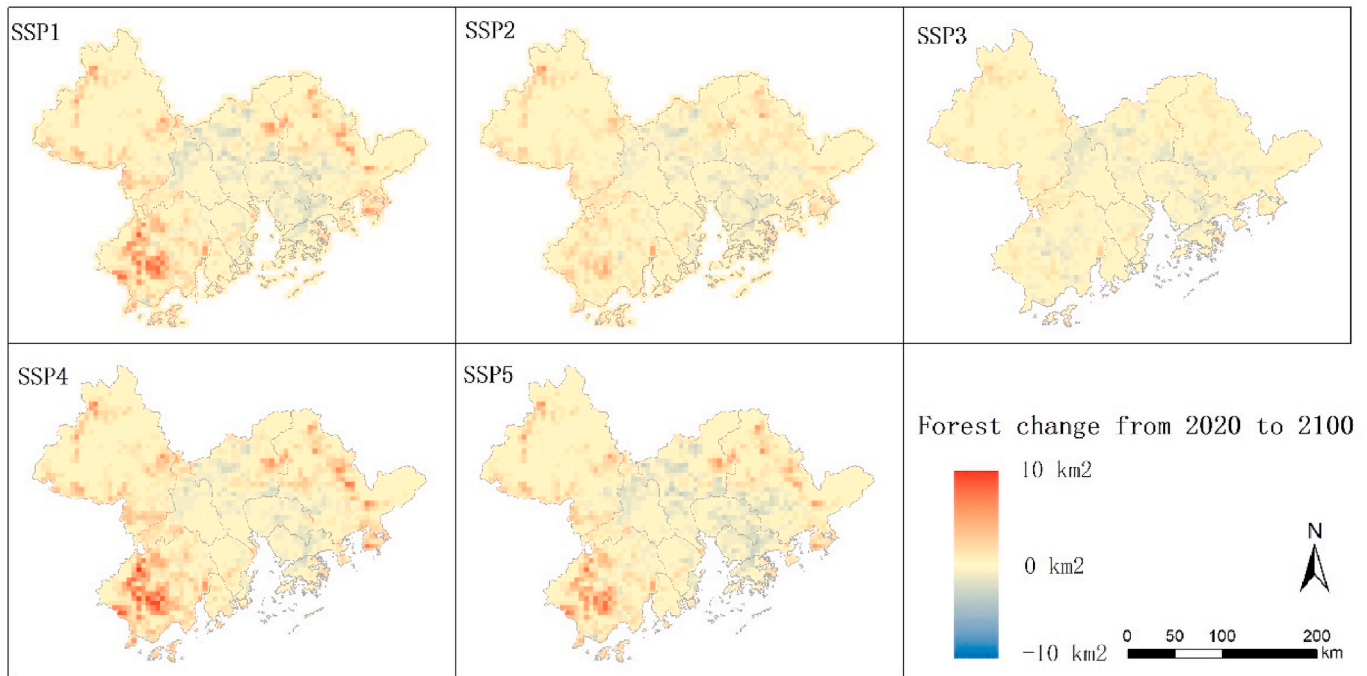


Fig. 7. Spatial changes of forest (LCZ A&B) under different SSPs from 2020 to 2100.

level changes in the urban LCZs (LCZ1–10) in the GBA (Table 3). Table 3 shows the differences in the development of urban LCZs in cities with different development levels. The growth of LCZ 1–4 (compact building and open high-rise building) is more clearly dominated in the central cities (Guangzhou, Shenzhen, Dongguan, and Foshan). The growth of LCZ 6–9 (open/lightweight/large low-rise building and sparse building) is more concentrated in fringe cities (Huizhou, Jiangmen, and

Zhaoqing), which have relatively low urbanisation degrees in the current. Simultaneously, Guangzhou, the city with the largest urban area in the GBA, has a significant increase in LCZ 6 & 7 because it contains some districts with a relatively low urbanisation rate. LCZ 5 & 10 (open mid-rise and heavy industry) changes are smaller than other urban LCZs. It is worth noting that the LCZ 7 (lightweight low-rise) in Shenzhen and Dongguan has decreased significantly, which indicates that the urban

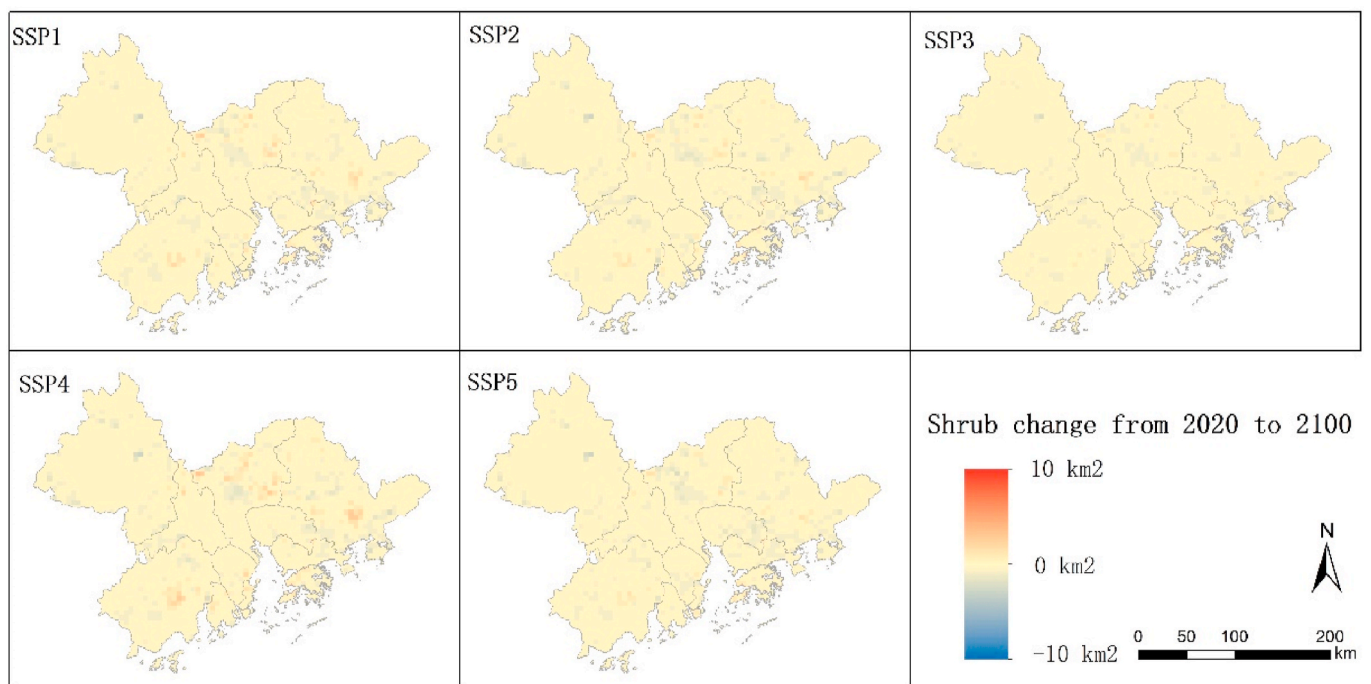


Fig. 8. Spatial changes of shrubs (LCZ C) under different SSPs from 2020 to 2100.

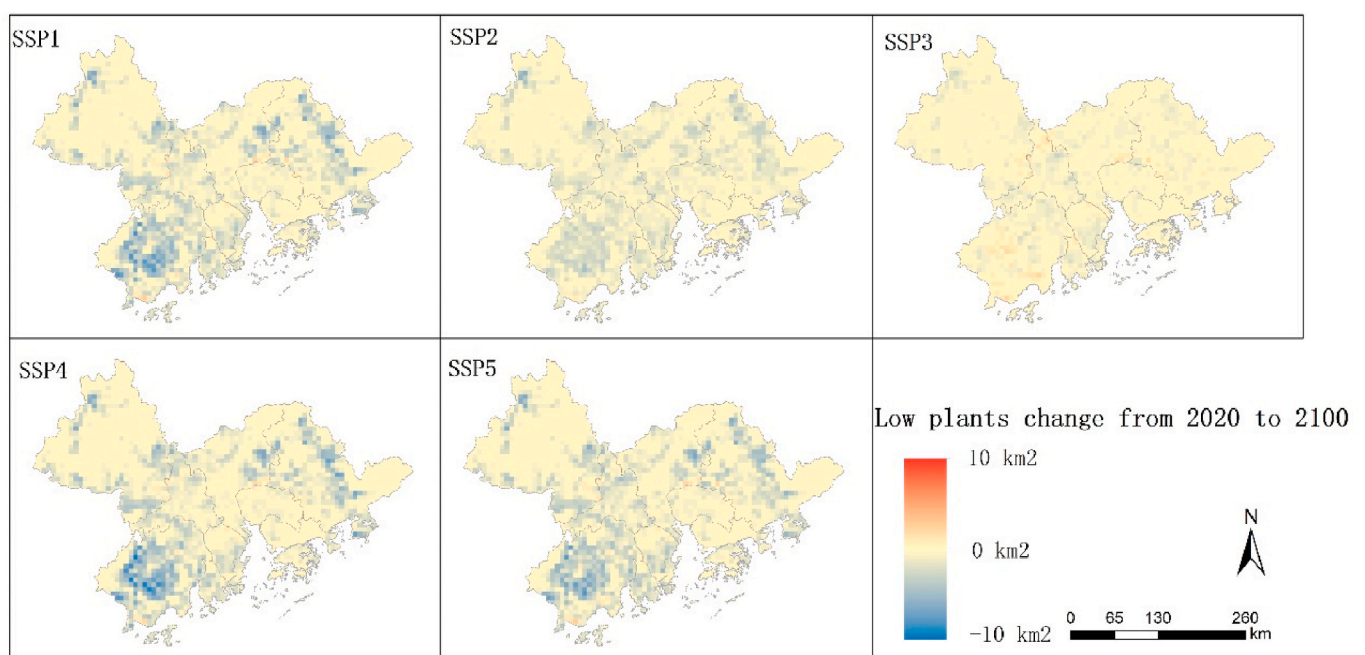


Fig. 9. Spatial changes of low plants (LCZ D) under different SSPs from 2020 to 2100.

landscape upgrade process of these two cities may be ahead of other cities.

3.4. Impact of ecological control line policy on land-use change

The simulation results shown above do not consider the ecological control line. Therefore, in this case, the urban land expansion will inevitably encroach on ecological lands (LCZ A–H). We counted the encroachment on each city's ecological lands in GBA by urban land through the ecological control line data (see Table 4). The extent of encroachment on ecological lands is positively correlated with urban

expansion's intensity under each SSP. As the largest city in the GBA region, Guangzhou suffers the most encroachment on ecological lands without ecological control lines. As one of the first-tier cities of the GBA, Shenzhen has fewer encroached ecological land areas because it has more hilly and mountainous areas that are difficult to be encroached by urban expansion. It should be noted that Jiangmen and Huizhou, two cities with relatively backward economic development, may face significant pressure of encroachment on their ecological lands in the future.

Furtherly, we explored the type of LCZ corresponding to the ecological lands occupied by urban expansion within the ecological control line (see Table 5). In other words, assuming 100% strict

Table 3

The area change of urban (LCZ1–10) in each city in the GBA from 2020 to 2100 in SSP2 (unit: km [2]).

	Guangzhou	Shenzhen	Dongguan	Foshan	Zhongshan	Zhuhai	Huizhou	Jiangmen	Zhaoqing	Hong Kong	Macao
LCZ1	27.51	39.4	31.22	20.36	9.07	6.7	16.7	6.83	3.09	7.75	1.28
LCZ2	29.77	27.49	38.59	29.83	14.16	5.77	13.91	12.94	5.37	1.9	0.18
LCZ3	64.54	10.83	47.61	52.08	23.03	14.16	41.1	33.45	19	8.62	0.02
LCZ4	60.23	27.51	48.51	61.9	30.18	12.45	20.36	18.18	8.92	14.09	0.75
LCZ5	4.6	-0.3	-0.26	3.48	3.58	9.43	9.14	10.68	3.99	2.75	0.12
LCZ6	97.74	14.73	22.56	3.09	-0.29	0.97	94.22	37.88	27.82	0.66	-0.21
LCZ7	47.18	-13.55	-21.03	13.07	2.22	6.79	35.38	152.14	56.67	-1.19	-0.14
LCZ8	14.6	-4.89	3.64	37.63	21.06	19.06	11.67	37.94	10.84	-0.3	1.54
LCZ9	-8.26	11.07	2.36	-2.28	-1.63	0.39	57.06	18.48	10.74	2.32	0.06
LCZ10	11.37	-3.14	5.01	-1.91	3.15	18.61	-0.91	4.15	1.77	1.07	0.71

Table 4

Urban expansion encroaches on ecological land in GBA's cities without the constraints of ecological control lines (km [2]).

	SSP1	SSP2	SSP3	SSP4	SSP5
Guangzhou	590.27	563.34	524.55	543.89	628.30
Shenzhen	43.18	41.24	38.25	39.90	47.83
Dongguan	280.36	271.55	256.12	264.32	291.27
Foshan	163.33	158.16	151.09	154.98	170.70
Zhongshan	146.69	142.12	133.92	138.05	154.96
Zhuhai	30.49	29.12	27.25	27.92	33.83
Huizhou	470.23	450.29	421.47	436.07	494.47
Jiangmen	581.60	554.52	518.56	536.04	618.49
Zhaoqing	266.79	255.64	243.09	249.62	280.48
Hong Kong	22.04	21.38	20.33	20.86	23.24
Macao	0.04	0.04	0.04	0.04	0.04

Table 5

The ecological land in the GBA that is free from being invaded by urban expansion under the constraints of the ecological control line in each scenario (km [2]).

LCZ	SSP1	SSP2	SSP3	SSP4	SSP5
A	108.28	79.15	50.97	82.85	144.08
B	81.09	52.31	32.21	63.12	97.96
C	116.24	91.44	57.15	86.23	135.32
D	289.2	269.34	213.62	187.38	375.59
E	10.81	9.36	7.64	8.47	12.75
F	8.45	6.79	5.01	5.97	9.84

implementation of the ecological control line, these ecological lands will be preserved. From a scenario perspective, implementing the ecological control line policy in SSP5 can protect more ecological land from urban expansion, which illustrates the importance of implementing the ecological control line policy in SSP5. On the other hand, under the ecological control line policy, LCZ D (low plants) benefits the most, mainly farmland. LCZ C (shrub) and LCZ A (dense trees) can also be well protected under the implementation of the ecological control line policy.

Due to spatial heterogeneity, the benefits of implementing the ecological control line policy in different cities are different. Table 6 counts the proportion of ecological land protected in each city due to the implementation of the ecological control line. It shows that in the SSP5, where urban expansion is the most intense, the ecological control line plays the most significant role in protecting ecological lands. The protection is most evident in Dongguan. In Dongguan, approximately 50% of the ecological control line area is protected by implementing the ecological control line policy. In Guangzhou, Shenzhen, Foshan, Zhongshan, and Jiangmen, the ecological control line's protective effects are also evident, reaching 10%–20%. In other words, ecological land protection in most cities in GBA will be significantly improved due to the implementation of the ecological control line policy.

Therefore, we simulated the future LCZ changes of each SSP scenario again, considering the ecological control line constraints. By overlaying the previous simulation results without ecological control line

Table 6

Ecological lands that preserved in each city due to the ecological control line policy by 2100.

City	Ecological lands preserved due to the ecological control line policy (%)				
	SSP1	SSP2	SSP3	SSP4	SSP5
Guangzhou	16.51	15.76	14.67	15.21	17.57
Shenzhen	10.15	9.69	8.99	9.38	11.24
Dongguan	50.30	48.72	45.95	47.42	52.26
Foshan	14.95	14.48	13.83	14.19	15.63
Zhongshan	20.77	20.12	18.96	19.55	21.94
Zhuhai	5.23	5.00	4.68	4.79	5.80
Huizhou	6.87	6.58	6.16	6.37	7.22
Jiangmen	13.12	12.51	11.69	12.09	13.95
Zhaoqing	2.48	2.38	2.26	2.32	2.61
Hong Kong	4.57	4.43	4.21	4.32	4.82
Macao	2.13	2.13	2.13	2.13	2.13

constraints, it can clearly show how the ecological control line protects ecological lands. Figs. 8 and 9 show the protective effects of the ecological control line through typical areas. The red grids represent the ecological land that will be occupied by urban land in the future without the constraints of the ecological control line. In the simulation of considering the constraints of ecological control lines, this part of ecological lands is protected. Meanwhile, the parts of the urban expansion blocked by the ecological control line will be transferred to other places, as the blue grids in Figs. 10 and 11.

Fig. 10 shows the core urban area of Dongguan, which is an important big city located in the central area of GBA. It can be seen that under the constraints of the ecological control line, the scattered ecological land within the core urban area is preserved in the process of urban expansion. Instead, the new urban land is transferred to the city's fringe in a scattered manner. For comparison, Fig. 11 shows the situation in Jiangmen, a city relatively far from the GBA center. Its main urban area is relatively small, and there is almost no ecological land inside. Without the constraint of the ecological control line, new urban land here invades many surrounding ecological lands within the ecological control line (red grids). However, under the constraint of the ecological control line, the urban expansion would be guided in the appropriate direction of reducing the impact on ecological lands.

4. Discussion

Our results show the impact of SSP scenarios on LCZ changes. In SSP5 and SSP1, urban (LCZ 1–10) expansion is the most evident due to rapid economic development and relatively large population growth. In the SSP3 with the slowest economic development, urban expansion is the least. In the SSP4, the rapid expansion of forest (LCZ A&B) is in sharp contrast with other scenarios because the GBA can adopt the reforestation policy as the developed area does in this divided pathway. Moreover, the trajectories of other land types in the GBA in each SSP show a negative correlation with urban and forest trajectories. On the one hand, the results prove the leading role of urban expansion, which is closely

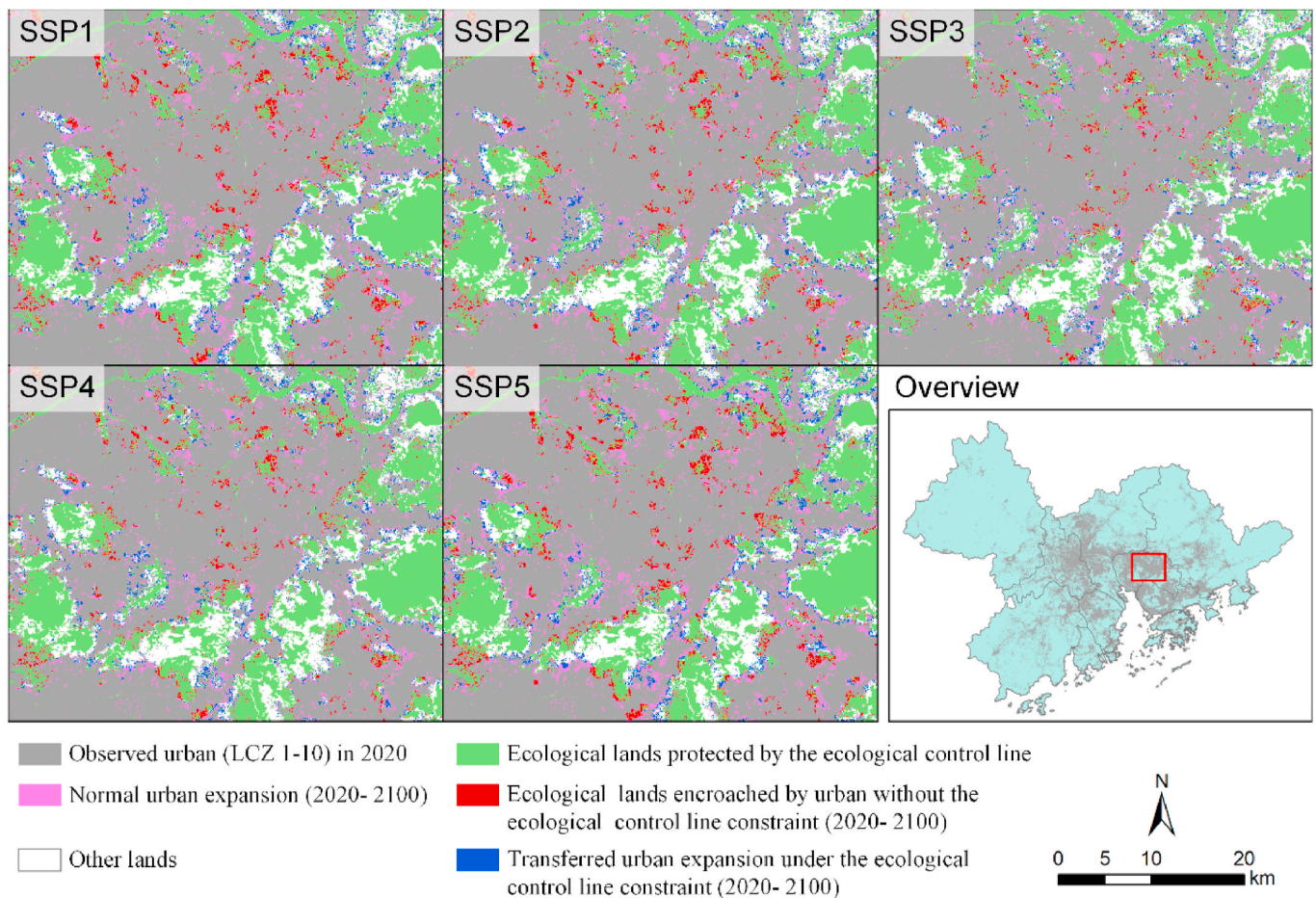


Fig. 10. The protective effect of the ecological control line on ecological lands in Dongguan from 2020 to 2100.

related to human activities, in the land change of GBA. On the other hand, the results also show that ecological management measures such as reforestation play a vital role in GBA's ecological landscape represented by forest.

The simulation results also illustrate the difference in land response between central cities and fringe cities. On the one hand, the difference is reflected in the dominant types of land change. In central cities, such as Guangzhou, Shenzhen, and Hong Kong, urban land plays an absolute leading role. That means only urban land in the central cities increases in each SSP, while other land types decrease due to urban expansion. However, in the fringe cities, such as Huizhou, Jiangmen, and Zhaoqing, land change is dominated by both urban land and forest. Even in some scenarios, the forest grows more than urban land. That means the fringe cities have assumed more ecological functions. On the other hand, the difference is also reflected in the changes in urban LCZs (LCZ 1–10). Some urban LCZs related to high-level urbanisation, such as LCZ 1–4, tend to grow in central cities. Simultaneously, some urban LCZs related to primary urbanisation, such as LCZ 6–9, tend to expand in fringe cities. The different land responses indicate that cities in the GBA with different development levels will face various land change challenges, even when facing the same scenario. It is still necessary to formulate land management and urban planning policies according to local conditions in the context of the coordinated development of the GBA.

There is a significant effect to implement the ecological control line. Ecological land protection in most cities in GBA will be significantly improved due to the implementation of the ecological control line policy. Nevertheless, at the same time, this effect also reflects the difference between central cities and fringe cities. In central cities, ecological control lines can protect the scattered ecological land within the built-up

area from being encroached on urban land. Therefore, this can better maintain the city's ecological landscape, conducive to realising Park City and Urban Sustainability concepts. However, in fringe cities, the role of ecological control lines is different. They have smaller built-up areas and not much internal ecological land. Therefore, ecological control lines' role is more reflected in guiding urban expansion to the appropriate direction, rather than encroaching on surrounding ecological land.

The data set we created in this study has many potential applications. First, it can be applied to policy impact assessment under the SSPs. It explores the land response of different policies in the SSPs with relatively fine resolution. Second, it can be used to explore urban land management under the SSPs. The simulation under the constraints of ecological control lines shows the impact of land management on urban expansion. Third, it can be used for research on urban climate. It uses the LCZ classification, which includes detailed urban land types. Therefore, urban climate researchers can obtain more relevant information from this set of data.

There are some limitations to this study. First, we used the same spatial driving factors when simulating future land changes under different scenarios due to data availability. Second, due to the lack of forecast data and models, we did not establish a particular land demand forecast model for the GBA. As a compromise, we used China's trend to apply to the GBA because they all belong to the middle and above units in their respective scales. Third, due to the current difficulty in obtaining time-series comparable LCZ maps, in this study, we did not perform a commonly adopted historical simulation of the LCZ spatial simulation model to verify its accuracy, but a compromised AUC test instead. Fourth, we did not consider the impact of climate on land change, which

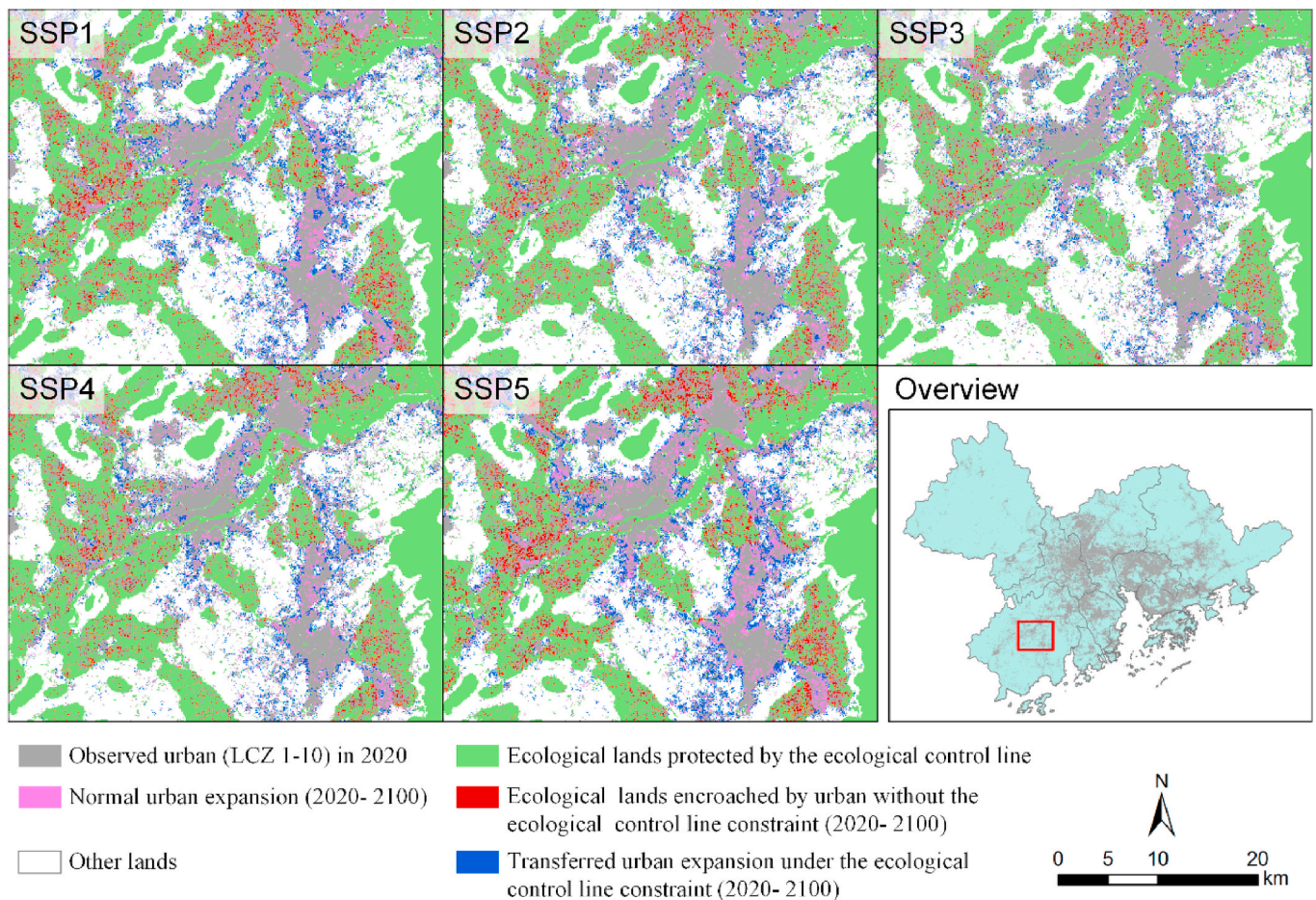


Fig. 11. The protective effect of the ecological control line on ecological lands in Jiangmen from 2020 to 2100.

may restrict the use of ecological land types in this data set.

5. Conclusion and future work

There are three significant advances in this study. First, this should be the first work to carry out simulations of future LCZ distributions in the context of SSP scenarios, which will directly serve researchers with urban climate as LCZ is one of their most popularly used land use land cover data in climate studies. Second, in contrast to previous future land-use simulations that have treated urban land (impervious surface) as a whole, our product depicted fine land change within the city due to the adaptation of the LCZ classification. Such detailed land change information of inner city could be useful for intra-urban variation related studies. Third, we explored the impact of land management policy (ecological control line) implementation on LCZ distribution. These advances can be embodied in many potential applications. For example, LCZ classification can provide more detailed information on land types, especially in the inner city. The simulation that includes a wealth of urban land types can provide more support for urban planning. Moreover, the definition of LCZ type is closely related to the physical characteristics of the land surface, such as roughness, albedo and anthropogenic heat output [30]. These physical characteristics information can better serve climate researchers.

In this study, we first created a data set of 2020 LCZ classification of the GBA with an overall accuracy of 94.4%. Then, we implemented simulations of LCZ changes for a 10-year time interval from 2020 to 2100 under SSPs with an AUC average accuracy of 0.744. The results show that there are differences in land response between central cities and fringe cities. In central cities, the urban-type LCZ dominates the

LUCC, i.e., urban-type LCZ is almost always the only growing land type in each SSP. In contrast, in fringe cities, both forest and urban-type LCZ grow, and even forest grows more rapidly. Moreover, more urban growth of compact and high-rise types (LCZ 1–4) in central cities, while the fringe cities have undertaken more urban development of mid-rise and low-rise types (LCZ 6–9) and forest LCZ.

Furthermore, we explored the impact of the ecological control line policy on land change. The results show that the implementation of ecological control line can be more effective in protecting ecological land (8.99%–52.26%) in central cities under the SSPs but slightly less efficient in protecting fringe cities (2.26%–13.95%). Moreover, the central city's ecological control line can better protect the ecological land within the built-up area, which is conducive to constructing a good ecological landscape. In fringe cities, the ecological control line can guide urban expansion in the appropriate direction to protect critical ecological resources.

In our future work, we will establish a particular land demand forecasting model for the GBA when more detailed forecast data under the SSP scenarios are available. The detailed spatial forecast data allows us to update the spatial driving factors of the land simulation to improve the simulation results' interpretability. Furthermore, as historical LCZ data are refined in the future, we can carry out historical LCZ simulations to more fully validate the performance of the FLUS model in simulating LCZ changes. Besides, based on this study's products, we will explore urban climate changes in different future scenarios, considering land feedback.

Declaration of competing interest

We declare that we do not have any commercial or associative interest that represents a conflict of interest in connection with the work submitted.

Acknowledgements

This research is supported by a Seed Funding for Strategic Interdisciplinary Research Scheme (Project no.: 102009942) from the University of Hong Kong. We are very grateful to the editor and the anonymous reviewers for their valuable comments and feedback, which substantially improved this article.

Appendix A. Supplementary data

Supplementary data to this article can be found online at <https://doi.org/10.1016/j.buildenv.2021.108077>.

References

- R.K. Pachauri, et al., Climate Change 2014: Synthesis Report. Contribution of Working Groups I, II and III to the Fifth Assessment Report of the Intergovernmental Panel on Climate Change, IPCC, 2014.
- D.X. Tran, et al., Characterizing the relationship between land use land cover change and land surface temperature, *ISPRS J. Photogramm.* 124 (2017) 119–132.
- H.D. Matthews, A.J. Weaver, K.J. Meissner, N.P. Gillett, M. Eby, Natural and anthropogenic climate change: incorporating historical land cover change, vegetation dynamics and the global carbon cycle, *Clim. Dynam.* 22 (2004) 461–479.
- K.L. Findell, et al., The impact of anthropogenic land use and land cover change on regional climate extremes, *Nat. Commun.* 8 (2017) 1–10.
- V. Huber, I. Neher, B.L. Bodirsky, K. H O Fner, H.J. Schellnhuber, Will the world run out of land? A Kaya-type decomposition to study past trends of cropland expansion, *Environ. Res. Lett.* 9 (2014) 24011.
- D. Byerlee, J. Stevenson, N. Villoria, Does intensification slow crop land expansion or encourage deforestation? *Global food security* 3 (2014) 92–98.
- M. Flannigan, et al., Global wildland fire season severity in the 21st century, *For. Ecol. Manag.* 294 (2013) 54–61.
- T.R. Pearson, S. Brown, L. Murray, G. Sidman, Greenhouse gas emissions from tropical forest degradation: an underestimated source, *Carbon Bal. Manag.* 12 (2017) 3.
- P. Meyfroidt, E.F. Lambin, Global forest transition: prospects for an end to deforestation, *Annu. Rev. Environ. Resour.* 36 (2011).
- U.N. Transforming, Our World: the 2030 Agenda for Sustainable Development, United Nations, New York, 2015.
- C.P.C. Report, On Work of the 18th Central Committee of the CPC in the 19th CPC National Congress: the Communist Party of China, CPC, 2017.
- K.C. Clarke, S. Hoppen, L. Gaydos, A self-modifying cellular automaton model of historical urbanization in the San Francisco Bay area, *Environ. Plann. Plann. Des.* 24 (1997) 247–261.
- A. Letourneau, P.H. Verburg, E. Stehfest, A land-use systems approach to represent land-use dynamics at continental and global scales, *Environ. Model. Software* 33 (2012) 61–79.
- J. He, et al., A counterfactual scenario simulation approach for assessing the impact of farmland preservation policies on urban sprawl and food security in a major grain-producing area of China, *Appl. Geogr.* 37 (2013) 127–138.
- X. Li, X. Zhang, A. Yeh, X. Liu, Parallel cellular automata for large-scale urban simulation using load-balancing techniques 24 (2010) 803–820.
- H. Oguz, A.G. Klein, R. Srinivasan, Using the SLEUTH urban growth model to simulate the impacts of future policy scenarios on urban land use in the Houston-Galveston-Brazoria CMSA, *Res. J. Soc. Sci.* 2 (2007) 72–82.
- A. Rahimi, A methodological approach to urban land-use change modeling using infill development pattern—a case study in Tabriz, Iran, *Ecological Processes* 5 (2016).
- Y. Yao, et al., Simulating urban land-use changes at a large scale by integrating dynamic land parcel subdivision and vector-based cellular automata, *Int. J. Geogr. Inf. Sci.* 31 (2017) 2452–2479.
- B.C. O'Neill, et al., A new scenario framework for climate change research: the concept of shared socioeconomic pathways, *Climatic Change* 122 (2014) 387–400.
- K. Riahi, et al., The Shared Socioeconomic Pathways and their energy, land use, and greenhouse gas emissions implications: an overview, *Global Environ. Change* 42 (2017) 153–168.
- D.P. van Vuuren, et al., Energy, land-use and greenhouse gas emissions trajectories under a green growth paradigm, *Global Environ. Change* 42 (2017) 237–250.
- S. Fujimori, et al., SSP3: AIM implementation of shared socioeconomic pathways, *Global Environ. Change* 42 (2017) 268–283.
- O. Fricko, et al., The marker quantification of the Shared Socioeconomic Pathway 2: a middle-of-the-road scenario for the 21st century, *Global Environ. Change* 42 (2017) 251–267.
- K. Calvin, et al., The SSP4: a world of deepening inequality, *Global Environ. Change* 42 (2017) 284–296.
- E. Kriegler, et al., Fossil-fueled development (SSP5): an energy and resource intensive scenario for the 21st century, *Global Environ. Change* 42 (2017) 297–315.
- A. Popp, et al., Land-use futures in the shared socio-economic pathways, *Global Environ. Change* 42 (2017) 331–345.
- G.C. Hurtt, et al., Harmonization of global land-use change and management for the period 850–2100 (LUH2) for CMIP6, *Geosci. Model Dev. Discuss. (GMDD)* (2020) 1–65.
- G. Chen, et al., Global projections of future urban land expansion under shared socioeconomic pathways, *Nat. Commun.* 11 (2020) 512–537.
- W. Liao, et al., Projections of land use changes under the plant functional type classification in different SSP-RCP scenarios in China, *Sci. Bull.* (2020).
- I.D. Stewart, T.R. Oke, Local climate zones for urban temperature studies, *Bull. Am. Meteorol. Soc.* 93 (2012) 1879–1900.
- B. Bechtel, et al., Generating WUDAPT Level 0 data—Current status of production and evaluation, *Urban climate* 27 (2019) 24–45.
- M. Demuzere, B. Bechtel, G. Mills, Global transferability of local climate zone models, *Urban climate* 27 (2019) 46–63.
- R. Avissar, Potential effects of vegetation on the urban thermal environment, *Atmos. Environ.* 30 (1996) 437–448.
- S.C. China, Outline Development Plan for the Guangdong-Hong Kong-Macao Greater Bay Area: the CPC Central Committee, The State Council of China, 2019.
- H.K.T.D.C. Featured, Statistics of the Guangdong-Hong Kong-Macao Greater Bay Area, 2020, 2020-07-06 [cited 2020/8/13] Available from: <https://research.hktdc.com/en/article/MzYzMDU5NzQ5>.
- G. Wen, Guangdong-Hong Kong-Macao Greater Bay Area Yearbook 2018: Guangdong-Hong Kong-Macao Greater Bay Area Yearbook Compilation Committee, 2018.
- K.C. Clarke, L.J. Gaydos, Loose-coupling a cellular automaton model and GIS: long-term urban growth prediction for San Francisco and Washington/Baltimore, *Int. J. Geogr. Inf. Sci.* 12 (1998) 699–714.
- X. Li, et al., A new global land-use and land-cover change product at a 1-km resolution for 2010 to 2100 based on human–environment interactions, *Ann. Assoc. Am. Geogr.* 107 (2017) 1040–1059.
- K.C. Seto, B. Guneralp, L.R. Hutyra, Global forecasts of urban expansion to 2030 and direct impacts on biodiversity and carbon pools, *Proc. Natl. Acad. Sci. Unit. States Am.* 109 (2012) 16083–16088.
- T.L. Sohl, M.C. Wimberly, V.C. Radeloff, D.M. Theobald, B.M. Sleeter, Divergent projections of future land use in the United States arising from different models and scenarios, *Ecol. Model.* 337 (2016) 281–297.
- X. Liang, et al., Delineating multi-scenario urban growth boundaries with a CA-based FLUS model and morphological method, *Landsc. Urban Plann.* 177 (2018) 47–63.
- L.C.H. Chung, J. Xie, C. Ren, Improved machine-learning mapping of local climate zones in metropolitan areas using composite Earth observation data in Google Earth Engine, *Build. Environ.* 199 (2021) 107879.
- L. Breiman, Random forests, *Mach. Learn.* 45 (2001) 5–32.
- B. Bechtel, et al., Mapping local climate zones for a worldwide database of the form and function of cities, *ISPRS Int. J. Geo-Inf.* 4 (2015) 199–219.
- D.M. Lawrence, et al., The land use model Intercomparison Project (LUMIP) contribution to CMIP6: rationale and experimental design, *Geosci. Model Dev. (GMD)* 9 (2016) 2973–2998.
- G.P. Kyle, et al., GCAM 3.0 Agriculture and Land Use: Data Sources and Methods: Pacific Northwest National Lab.(PNNL), 2011. Richland, WA (United States).
- N. Dong, L. You, W. Cai, G. Li, H. Lin, Land use projections in China under global socioeconomic and emission scenarios: utilizing a scenario-based land-use change assessment framework, *Global Environ. Change* 50 (2018) 164–177.
- X. Liu, et al., A future land use simulation model (FLUS) for simulating multiple land use scenarios by coupling human and natural effects, *Landsc. Urban Plann.* 168 (2017) 94–116.
- P.H. Verburg, P.P. Schot, M.J. Dijst, A. Veldkamp, Land use change modelling: current practice and research priorities, *Geojournal* 61 (2004) 309–324.